A98-31520

ICAS-98-2,8,2

# PREDICTION OF THE VORTICITY FIELD PRODUCED BY AIR-JET VORTEX GENERATORS

by Tim P Bray* & Kevin P Garry†
College of Aeronautics, Cranfield University,
Bedford, MK43 0AP.
United Kingdom

## Abstract

A parametric study of the vorticity profiles of air-jet vortex generators has been carried out, and an empirical model which allows the prediction of the vorticity field downstream of the air-jet vortex generators has been derived.

Measurements were carried out in two studies: a low speed and a high speed test. The low speed test was at a free-stream velocity of 20 m/s (M = 0.588), while the high speed test was at Mach numbers of 0.5, 0.6, 0.75. Both tests used a miniature 5 hole pressure probe traversed in a plane normal to the free-stream, downstream of the vortex generators.

The air-jets were all of circular jet profile. The jet variables were tested as follows: jet pitch as $30° < \alpha < 60°$; jet skew as $30° < \beta < 60°$, jet diameter-to-boundary-layer-thickness as $0.098 < D/\delta < 0.289$ and jet-to-free-stream velocity ratio as $0.7 < VR < 2.0$.

The experimental data has been used to produce a series of relationships which allow the prediction of vorticity from vortex generators with the aim of simplifying numerical simulations of a flow field incorporating such devices.

## Notation

| | |
|---|---|
| M | Mach number |
| MR | Mach number ratio ($=M_{jet}/M_\infty$) |
| R | Radius (m) |
| $U_\infty$ | Free-stream Velocity (m/s) |
| u, v, w | Local velocity vector component magnitudes (m/s) |
| V | Local velocity vector magnitude (m/s) |
| VR | Velocity ratio ($=V_{jet}/U_\infty$) |
| x, y, z | Co-ordinate system (m) |
| $\alpha$ | Jet incidence (°) |
| $\beta$ | Jet skew angle (°) |
| $\delta$ | Boundary layer thickness |
| $\omega$ | Vorticity (1/s) |

## Introduction

The use of highly curved S-ducts to facilitate engine-integration of future Low Observability (LO) or Advanced-Short-Take-Off and Vertical-Landing (ASTOVL) military aircraft is highly likely. However, the aerodynamic qualities of these intakes causes large total-pressure non-uniformity at the engine face, which is termed inlet total pressure *distortion*. The inlet distortion of an engine-inlet configuration is critical in optimising the propulsion performance, and should be as low as possible.

One method of reducing the inlet distortion is to introduce vortex generators (either conventional vanes, or air-jets) to the inlet to modify the development of the flow field. The use of vane vortex generators is well established for external flows, and these devices suffer from the problem of being passive. Air-jet vortex generators can be controlled, and have the further benefit of being able to be used in regions where the flow is separated, since the air-jet can penetrate the separated region and encourage mixing in the free shear layer.

The design and optimisation of an intake fitted with vortex generators is a difficult task, since the range of variable parameters is extremely large. Thus, both

---

* Research Engineer & Engineering Doctorate (EngD) Student

† Senior Lecturer, Flow Control & Prediction Group

wind tunnel testing and Full-Navier-Stokes (FNS) CFD solutions become expensive for the initial design of an intake.

One solution is to use a design code which solves the Reduced- (or parabolised) Navier-Stokes (RNS) equations, and thus reduces the CPU time required. A method to further reduce the grid complexity is to input the effects of the vortex generators, rather than model the generators themselves. Thus a vortex generator can be replaced by a step input in vorticity, of the correct amount, at the point where the vortex generator would be located. The code would then allow the vorticity to develop downstream, thus simulating the vortex. This reduces the grid complexity as well as the CPU time to evaluate the flow field.

In order to input the correct value of vorticity, a simple empirically based model or database of vorticity results for a range of vortex conditions is needed, and thus this paper describes the production of such a model.

## Experimental Method

Two series of tests were carried out in order to understand the characteristics of vortex generators. The first test was a low speed investigation, carried out in the Cranfield College of Aeronautics 'Brough' open return wind tunnel, at a free-stream speed of 20 m/s. This test was carried out to investigate the parameters associated with vortex generators without the influence of Mach number, thus reducing the cost of the total programme.

The second series of tests was carried out at a higher Mach number in the Cranfield College of Aeronautics 9" x &7½" (0.288 m x 0.19 m) transonic wind tunnel facility. These tests were designed to add the Mach number dimension to the database of results obtained from the first series of tests.

The results of both series of tests were compiled into a model of vortices produced by a number of air-jet vortex generators.

### Low Mach Number Tests

The Brough wind tunnel has a 2' x 2' (0.61 m x 0.61 m) working section of 2.4 m length. The working section floor has a natural turbulent boundary layer thickness ($\delta$) of 18 mm (at a location 0.8 m from the entrance to the working section, where the vortex generators were located) which was considered too small to obtain accurate measurements of an embedded vortex. Hence, the boundary layer was artificially thickened using three 2 mm diameter trips placed at 50 mm intervals across the entrance to the working section. These trips caused an increase on thickness to 41.5 mm while retaining a $^1/7$ power law profile across the working section.

The air-jet vortex generators were similar as those described by Selby[1], and were tested over a wide range of variables: jet incidence ($\alpha$ at 30°, 45° and 60°); jet skew ($\beta$ at 30°, 45° and 60°); jet velocity ratio ($VR$ at 0.7, 1.0, 1.3, 1.6 and 2.0), jet hole diameter ($D$ at 4 mm, 8 mm and 12 mm corresponding to $D/\delta$ of 0.09, 1.98, 2.89 respectively).

Measurements were made in a plane normal to the free-stream direction, at 4 streamwise locations (at 0.16 m, 0.5 m, 0.8 m and 1.1 m behind the vortex generator - $x/\delta$ = 3.86, 12.05, 19.28, 26.56 respectively) using a five hole pressure probe. The probe was traversed over a grid of points in the two cross-stream directions at intervals of 5 mm. At each point, the local total and static pressures were measured along with the local flow angle in pitch and yaw. From this, the local cross-stream velocity vectors could be derived, and by spacial differentiation in the cross-stream plane, the local vorticity.

### Errors and Repeatability

The five hole probe was calibrated over the pitch/yaw range ±32°, and the maximum errors in pitch and yaw angle were found to be 0.1°, with the maximum error in local flow dynamic pressure, 3%. This error translates to an absolute error in vorticity approximately 5 $s^{-1}$. The peak levels of vorticity were measured as up to three orders of magnitude larger.

The grid spacing was chosen as 5 mm, since this gave the largest number of data points in a grid for the optimum run time. Thus a grid of 300 data points would take approximately 1 hour, and would give sufficient data to allow an accurate interpolation of the data set. Repeatability in peak vorticity measurement was seen to be within 2%.

### High Mach Number Tests

The College of Aeronautics 9" transonic/supersonic wind tunnel is a facility which has interchangeable working sections which allow it to be used as a transonic facility (from Mach 0.45 to Mach 1.1) or as a supersonic facility (from Mach 1.2 to Mach 3.5). The wind tunnel is a sub-atmospheric continuous running facility with a variable stagnation pressure of between 3 psi and 12 psi, dependant on the desired Mach number and model blockage.

The transonic working section is 9" x 7½" (0.288 m x 0.19 m) and is fitted with slotted liners on the roof and floor of the tunnel with an open area ratio of

17.5%. The side walls of the tunnel are removable, and steel or glass doors are available. For this test, a new aluminium side wall was made, and was fitted with a circular window mounted on a thrust bearing. The centre of the window was fitted with a series of removable plugs which contained the vane and air-jet vortex generators.

Measurement of the vorticity was made by traversing a 1.75 mm diameter probe in one of four streamwise planes. Slits were cut in the tunnel wall to allow the probe to enter the tunnel working section, with the traverse mechanism mounted externally. This simplified the introduction of the traverse to the working section, and reduced the potential for blockage in the working section. The traverse was encased in a plenum chamber, access to which ws via slots in the working section wall, which were filled with brass inserts when not in use.

Since the working section of this tunnel was relatively small, it was important that the scale of the vortices was matched accordingly, while ensuring that they were large enough to make accurate measurements. It was decided that a boundary layer thickness of 20 mm would be a suitable scaling parameter, in order that there was not a significant reflection of the vortices on the tunnel walls. Further, since the tunnel walls either side of the vortex would be slotted, it was considered that this reflection would be less than for a solid walled tunnel. The boundary layer of the tunnel at the vortex generator station was thickened using a 3 mm trip located at the entrance to the working section, and the thickness was measured using a Preston tube. The boundary layer thickness was measured as 20.0 mm.

Air-jets were used as in the low speed test. Parameters tested were as follows: $D/\delta = 0.15, 0.3$; $\alpha = 30°, 45°, 60°$; $\beta = 30°, 45°, 60°$; $MR = 1.6$; $x/\delta = 8.75, 16.25, 23.75, 31.25$; $M_\infty = 0.45, 0.60, 0.75$.

As with the low speed tests, measurements of the local pitch & yaw and total and static pressures were taken, such that local Mach number components could be found. Using the tunnel total temperature (as measured in the settling chamber), the cross-stream velocity vectors could be found, and thus vorticity calculated.

### Errors and Repeatability

The 1.75 mm five hole probe was calibrated (over the pitch/yaw range ±24°) in the DERA Bedford 4" (101.6 mm) tunnel at Mach numbers from 0.3 to 0.7 in 0.1 steps. The probe was found to be Mach number insensitive within this measurement range. The maximum errors in the derived pitch and yaw angle were found to be 0.6°, with the maximum error in local Mach number of 3%. This error translates to an absolute error in vorticity approximately 300 $s^{-1}$. The peak levels of vorticity were measured as up to two orders of magnitude larger.

The grid spacing was chosen as 3 mm, since this gave the largest number of data points in a grid for the optimum run time. Thus a grid of 300 data points would take approximately 1 hour, and would give sufficient data to allow an accurate interpolation of the data set. Repeatability in peak vorticity measurement was seen to be within 3%.

## Results

The vorticity data measured from each experimental run was interpolated to map the vorticity for each vane air-jet configuration. This data then allows the generation of an empirical model.

From the vortex model proposed by Lamb[2], it is noted that the cross-sectional vorticity distribution for a vortex is Gaussian in nature, and can be written in the form:

$$\omega(r) = \omega_{peak} e^{-k\left(r/R_{0.5}\right)^2} \qquad (1)$$

where $\omega$ is the vorticity, $r$ is the radial distance from the centre of the vortex and $R_{0.5}$ is the Half-Life Radius of the vortex. The half-life radius is defined as the radial distance from the centre of the vortex where the local vorticity is half the peak value. Rearranging this equation with $\omega(r) = 0.5\omega_{peak}$ (where $r = R_{0.5}$), it is possible to prove that the value of $k$ is $ln(½)$ (=0.693). Thus, in order to define any vortex cross-section, only the peak vorticity and the half-life radius are needed. The empirical relationship should then link the physical parameters and the local flow conditions to these values.

## Discussion

The interpolated vorticity distributions for the air-jet cases were used as the basis for two empirical equations, one to describe the peak vorticity, and one to describe the half-life radius.

The equations were formed by assessing the trends in the experimental data. Since over 300 data points had been taken, the effect of varying any one parameter while holding all others constant could be investigated.

These equations are as follows:

$$\omega_{peak} = K_1[f]\left(\frac{x}{\delta}\right)^{K_2} M^{K_3}$$

where

$$f = \left\{ \begin{array}{l} \left\{ \begin{array}{l} \left[K_4 \cos(\alpha - K_5) + K_6\right]\beta \\ +K_7 \sin(\alpha - K_8) + K_9 \end{array} \right\} \left(VR.\frac{D}{\delta}\right) \\ +\left\{ \begin{array}{l} \left[K_{10} \sin(\beta + K_{11}) + K_{12}\right]\alpha \\ +K_{13} \cos(\beta + K_{14}) + K_{15} \end{array} \right\} (VR) \\ +\left\{ \begin{array}{l} \left[K_{16} \sin(\beta + K_{17}) + K_{18}\right]\cos(\alpha + K_{19}) \\ +K_{20} \sin(\beta + K_{21}) + K_{22} \end{array} \right\} K_{23}\left(\frac{D}{\delta}\right) \\ +\left\{ \begin{array}{l} \left[K_{24} \sin(\beta + K_{25}) - K_{26}\right]\alpha \\ K_{27} \sin(\beta + K_{28}) + K_{29} \end{array} \right\} \end{array} \right\} \quad (2)$$

$$R_{0.5} = \left\{ \begin{array}{l} \left[L_1 \sin(\alpha) + L_2\right]\left[L_3 \sin(\beta) + L_4\right] \\ \left[L_5 MR + L_6\right]\left[L_7 \frac{D}{\delta} + L_8\right] \\ \left[L_9 \frac{x}{\delta} + L_{10}\right]\left[L_{11} M + L_{12}\right] \end{array} \right\} \quad (3)$$

Clearly, the cross-product terms in this equation highlight the complexity of the problem in producing a simple model. An optimiser algorithm was employed to interactively determine the values of $K_n$ and $L_n$ in the above equation. The convergence criterion were based on minimisation of the average modulus of the percentage error between the predicted value (i.e. that made by the above equation), and the measured value from experiment. The following equation results:

$$\omega_{peak} = 5.25[f]\left(\frac{x}{\delta}\right)^{-0.88} M^{1.33}$$

where

$$f = \left\{ \begin{array}{l} \left\{ \begin{array}{l} \left[2230\cos(\alpha - 0) - 580\right]\beta \\ +1000\sin(\alpha - 15) + 26700 \end{array} \right\} \left(VR.\frac{D}{\delta}\right) \\ +\left\{ \begin{array}{l} \left[8.4\sin(\beta + 15) - 19\right]\alpha \\ +2300\cos(\beta + 58) + 840 \end{array} \right\} (VR) \\ +\left\{ \begin{array}{l} \left[-6.2\sin(\beta + -26) - 0.2\right]\cos(\alpha + 51) \\ +9\sin(\beta + 81.5) - 12 \end{array} \right\} (6100)\left(\frac{D}{\delta}\right) \\ +\left\{ \begin{array}{l} \left[-0.661\sin(\beta + 30) + 38\right]\alpha \\ 2500\sin(\beta - 20) - 3100 \end{array} \right\} \end{array} \right\} \quad (4)$$

$$R_{0.5} = \left\{ \begin{array}{l} \left[\sin(\alpha) + 4.51\right]\left[1.3\sin(\beta) + 5.16\right] \\ \left[0.0689 MR + 0.536\right]\left[0.162\frac{D}{\delta} + 0.0893\right] \\ \left[0.0565\frac{x}{\delta} + 1.113\right]\left[0.0059 M + 0.0534\right] \end{array} \right\} \quad (5)$$

In order to assess the errors involved in these predictions, the experimental configurations were used as the input to these equations, and the results were plotted against the actual experimental values. The results are shown below:

**Figure 1: Accuracy of the Peak Vorticity Model**

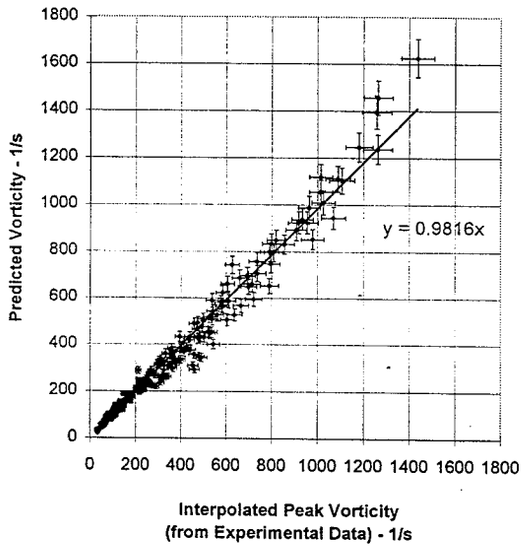


**Figure 2: Accuracy of the Radius Model**

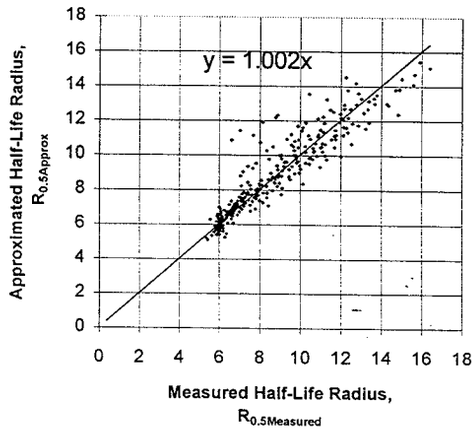


Both plots show that the accuracy is most acceptable in predicting these variables. However, it is necessary to consider their effect in the prediction of the entire vorticity profile. Below, a slice through a vorticity plot shows a typical result.

Figure 3: Vorticity profile Through a Vortex

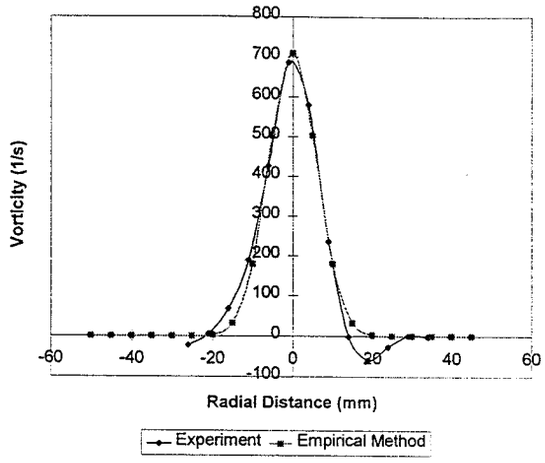


The estimation of peak vorticity is to within 10% at the 95% confidence level. The prediction of the half-life radius is to within 2 mm at the 95% confidence level.

## Limits of the models

The models are currently limited to the range of test conditions which have been completed to date. The limits for the air-jet cases were:

- $30° < \alpha, \beta < 60°$
- $0.1 < D/\delta < 0.3$
- $0.7 < MR < 2.0$
- $3.85 < x/\delta < 30$
- $0 \leq M_\infty < 0.75$

It is interesting to note that while these are the limits of the data used to construct the air-jet equations, comparisons with Compton & Johnston[3] have shown that the equation will hold for higher vales of $\beta$, $D/\delta$ and $x/\delta$ with the same degree of accuracy as for the present study's data. This suggests that the physical flow features hold for parameters just outside of those tested to produce this model, and thus allow the use of the empirical model to optimise the use of air-jet vortex generators, and to predict the significant trends in their use.

Figure 4: Comparison with Compton & Johnston

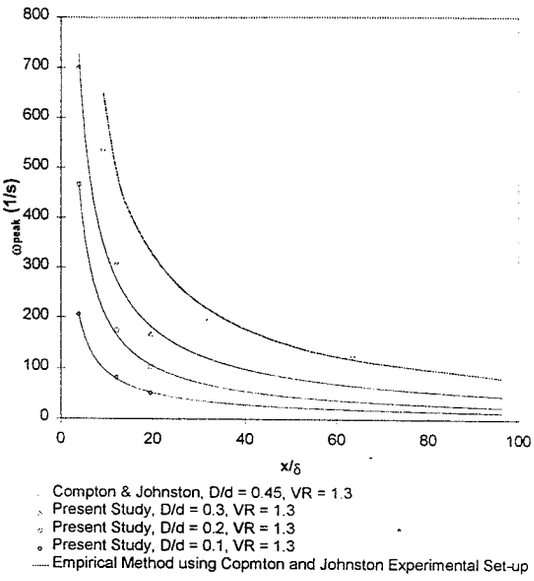


## Implications of the Air-Jet Model

Using the model for the air-jet vortex generators, it is possible to investigate the boundary conditions with respect to the variation of individual parameters. In almost all cases, the effect on the wall in the decay of the peak vorticity was not significant, and it is expected that this would occur at between 25 and 35 $x/\delta$, depending on the height of the vortex at generation.

In the figure below, it is may be seen that the effect of increasing the pitch angle of the jet is quite dramatic. Clearly, the maximum vorticity is reached with the pitch angle, $\alpha$, between 20° and 30°. It would appear that the exact angle for the maximum vorticity is a function of the skew angle, $\beta$, since, the optimum pitch angle appears to increase with increasing skew.

**Figure 5: Effect of Jet Pitch Angle (Model Prediction)**

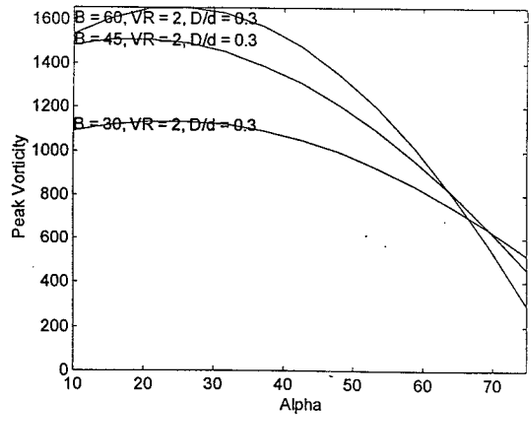

The effect of jet skew angle is depicted in the figure below. It is clear that the magnitude of the change in vorticity due to the skew angle is also a function of the pitch angle. In the case of a high pitch angle ($\alpha$ = 60°), the effect of changing the skew angle is small. However, as the pitch angle is reduced, the effect of changing the skew angle becomes more pronounced, and the maximum vorticity occurs with a skew angle of 60°.

**Figure 6: Effect of Jet Skew Angle (Model Prediction)**

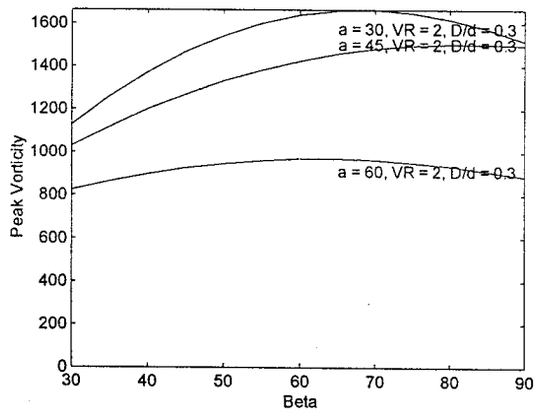


The effect of velocity ratio is shown below, and this plot has curves for varying hole diameter ratios. It is clear that the effect of velocity ratio is approximately linear (allowing for experimental error).

**Figure 7: Effect of Jet Velocity Ratio (Model Prediction)**

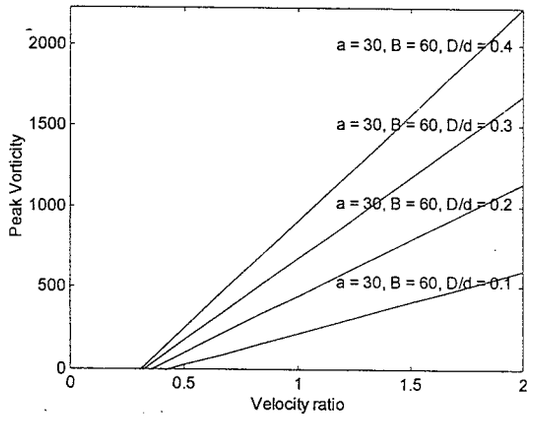


It would appear that there is a minimum velocity ratio for vortex production, and this limit is dependant on the jet diameter ratio. For a larger jet diameter ratio, the velocity ratio needed to sustain vortex production is less, which is consistent with momentum considerations.

The figure below illustrates the minimum jet diameter ratio needed to produce vorticity. Using a low velocity ratio (of 0.5), a hole diameter ratio of 0.07 is needed, but by increasing the velocity ratio, the hole diameter ratio can be reduced significantly in order to produce the same level of vorticity.

**Figure 8: Effect of Jet Sizing Ratio (Model Prediction)**

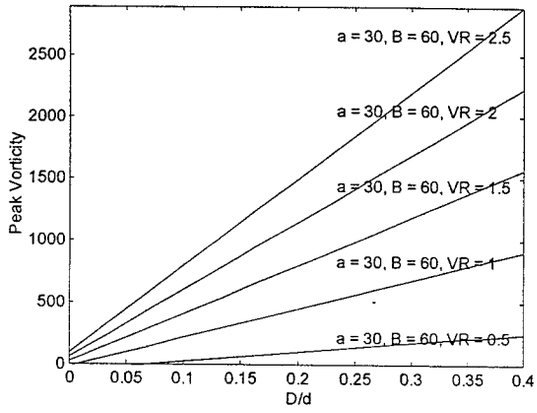


The effect of Mach number on the peak vorticity is shown, and it is clear that, the trend is that of a power law. The significance of this is that a large amount of high Mach number testing is unnecessary, since the low speed results can be extrapolated using this relationship. This would greatly reduce the cost of testing at higher Mach numbers.

**Figure 9: Effect of Mach Number (Model Prediction)**

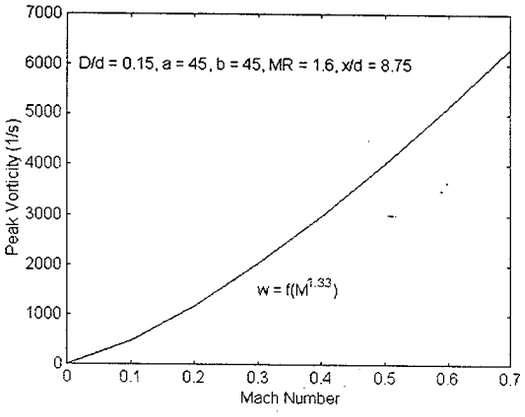


The plot below shows the effect of the downstream distance on the peak vorticity. It should be remembered that for a free vortex, the peak vorticity will decrease away from the point of generation, but the area integrated vorticity (or circulation) should remain constant. The same is true for the embedded vortex which is not significantly close to the wall. The decay which is seen below, is not that due to the significant reduction in the *total* vorticity, but merely due to the spreading out of the vorticity signature with the resulting reduction in peak vorticity.

**Figure 10: Streamwise Decay of Peak Vorticity (Model Prediction)**

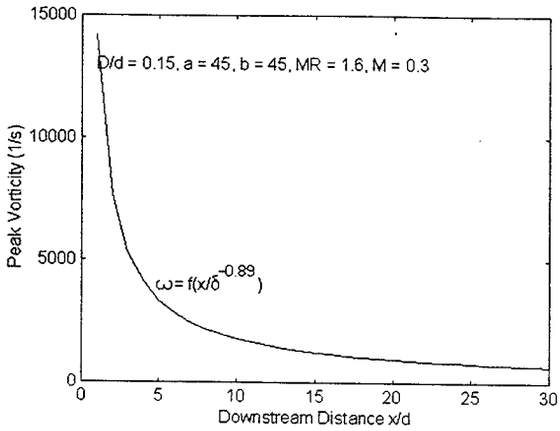


## Conclusions

Empirical models of the vorticity field have been deduced from a comprehensive experimental parametric study of both the vane and air-jet vortex generators.

The models predict the peak vorticity at any downstream location based on the geometric parameters of the vortex generator, and on the local flow conditions. Using this peak vorticity, the cross-stream vorticity distribution can also be found.

From this empirical model, the optimum configuration of vortex generators is easily derived. In addition, the equations are in a form which facilitates incorporation with flowfield numerical models.

## Acknowledgements

This programme of work was carried out with the support of the Defence Evaluation & Research Agency (DERA) Bedford, on behalf of the UK Ministry of Defence Procurement Executive.

## References

1 Selby, G. V., Lin, J. C. & Howard, F. G. Control of low-speed turbulent separated flow using jet vortex generators. Experiments in Fluids, pp 394-400, Vol. 12, No. 6, 1992.

2 Lamb, Sir H. Hydrodynamics. Cambridge University press, 1932. pp 591-592.

3 Compton, D. A. & Johnston, J. P. Streamwise vortex production by pitched and skewed jets in a turbulent boundary layer. AIAA Paper 91-0038.